

On the Structure of the Active Site of Ti-Silicalite in Reactions with Hydrogen Peroxide: A Vibrational and Computational Study

G. Tozzola,* M. A. Mantegazza,* G. Ranghino,* G. Petrini,* S. Bordiga,† G. Ricchiardi,†
C. Lamberti,† R. Zulian,† and A. Zecchina†,¹

* ENICHEM SpA, Centro di Ricerche di Novara, Via G. Fauser 4, Novara, Italy; and † Dipartimento di Chimica Inorganica,
Fisica e dei Materiali, Via P. Giuria 7 I-10125 Torino, Italy

Received June 4, 1997; revised June 2, 1998; accepted June 4, 1998

Ti-Silicalite (TS-1) is an excellent catalyst for the selective oxidation of alkenes to epoxides, of NH_3 to hydroxylamine and of the ammoximation of cyclohexanone, using H_2O_2 as oxidant. This paper reports spectroscopic (IR/Raman) and computational (HF, cluster models) studies on the complexes formed upon interaction of the Ti catalytic centre with water and hydrogen peroxide. Evidence is presented of the formation of unstable hydroperoxidic species upon interaction with neutral aqueous H_2O_2 solutions, which can be converted into a more stable ionic complex in a basic environment. The vibrational spectra of these complexes have been recorded in appropriately designed low-temperature experiments on solution-soaked powders bearing some resemblance with the catalytic reactor environment. The assignment of the spectra was confirmed by *ab initio* calculations and by parallel experiments on the structurally similar Ti-free silicalite. © 1998 Academic Press

INTRODUCTION

Since the discovery of the unique catalytic properties of Ti-Silicalite (TS-1) in selective oxidations using H_2O_2 as oxidizing agent (1–7), several attempts have been made to characterize by physical methods the electronic and coordinative state of titanium centres, before and after the interaction with various molecules playing a role in the catalytic reactions (H_2O , NH_3 , H_2O_2 , CH_3OH) (8–29). In particular: (i) Accurate XRD measurements have demonstrated that, in well synthesized TS-1 samples, the unit cell volume increases linearly with the Ti(IV) content (20), in good agreement with model equations for isomorphous substitution of Si with Ti at tetrahedral framework sites (1,8). (ii) A second fingerprint of this material is an IR band at 960 cm^{-1} , whose intensity is proportional to the Ti(IV) content (1,12). A band at similar frequency is also present in the Raman spectra (9). This band was originally assigned to the stretching mode of a titanyl group $(\text{SiO})_3\text{Ti}=\text{O}$, this assignment being later discarded because it could not ex-

plain the blue shift observed upon interaction with adsorbates like methanol and water (9,12–14,17). The most widely accepted assignment is now in terms of the ν_{as} of (SiOTi) groups. (iii) A third feature is represented by the oxygen to titanium charge transfer transition at 49.000 cm^{-1} characteristic of the Ti(IV) in tetrahedral environment (12–14). (iv) A fourth characteristic is the strong XANES peak at 4969 eV which is typical of Ti(IV) in tetrahedral coordination (13,14,24).

The effect observed upon interaction with adsorbates like H_2O , NH_3 , and CH_3OH is easily explained in terms of insertion of ligands in the coordination sphere of Ti(IV) centres, from tetrahedral to distorted octahedral coordination (with subsequent increase of the Ti-O bond length and increase of the Si-O stretching character of the ν_{as} of the (SiOTi) mode (9,17)). Further evidences of the propensity of the Ti centre to vary its coordination number in the presence of adsorbates have been obtained by means of UV-visible (12–15,17,19) and XANES (13,14,21–24) spectroscopies.

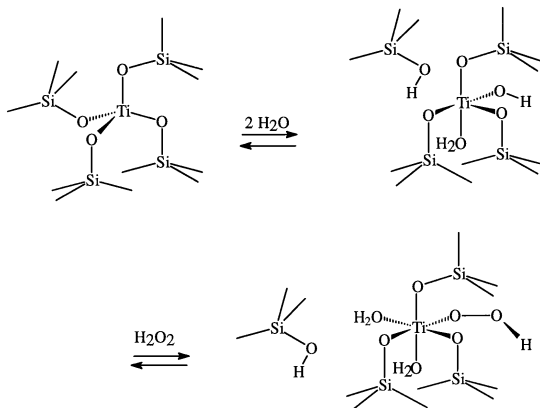
UV-visible spectroscopy gives also the simplest evidence on the formation of peculiar complexes on TS-1, upon H_2O_2 dosage. In fact, in the presence of a neutral H_2O_2 solution, the sample turns yellow because of the formation of a distinctive adsorption at 25800 cm^{-1} . The assignment of this band in terms of ligand-to-metal charge transfer of peroxo and or hydroperoxo complexes of Ti(IV), has been discussed elsewhere (15,17,19).

The absorption at 25800 cm^{-1} is remarkably labile and disappears in a few minutes at RT unless the sample is continuously fed with fresh H_2O_2 solution. Cooling to 230 K slows down the decomposition and the band can then be observed on the time-scale of hours. Upon interaction of the fresh catalyst with an aqueous $\text{NH}_3/\text{H}_2\text{O}_2$ solution, the characteristic band is formed at distinctly higher frequency (28500 cm^{-1}) and it is remarkably more stable (17). It is worth noticing that the spectrum obtained after dosage of the basic $\text{NH}_3/\text{H}_2\text{O}_2$ solution is identical to that obtained with $\text{NaOH}/\text{H}_2\text{O}_2$ solution. Moreover, the band at 28500 cm^{-1} can also be obtained from that at 25800 cm^{-1}

¹ Corresponding author. E-mail: ZECCHINA@CH.UNITO.IT.

by dosing NH_4OH or NaOH solutions to the species previously formed in neutral conditions (17).

These observations pointed to the hypothesis that two similar but not identical oxygen containing Ti(IV) complexes are formed in neutral and basic solutions and that the structure is not dependent upon the nature of the base (17). Moreover, the complex formed in neutral solutions can be converted into a more stable form in basic solutions. A possible scheme illustrating the reactivity of Ti centres with water and H_2O_2 solution is represented below.



However, only on the basis of UV-visible data, the exact structure of this key species has never been completely elucidated and some debate is still open (8,11,15,17,19,27,28).

For this reason a specific study on the vibrational properties of the Ti-peroxo complex has been undertaken and new IR and Raman data on the complexes formed in presence of H_2O_2 , together with *ab-initio* Hartree Fock calculations on cluster models supporting the spectroscopical assignments, will be presented in this paper. Due to difficulties encountered in the dosage of H_2O_2 from the gas phase, the spectra were obtained on the TS-1 sample impregnated with H_2O_2 solutions. Since the industrial TS-1 catalysts operates in solution, the presence of the soaking solution makes the catalytic system investigated by Raman and IR spectroscopies very close to the real catalytic one. Due to the instability of the peroxo species at RT, both Raman and IR spectra have been obtained at low temperature (about 230 K). However, while the Raman spectra at 230 K of samples impregnated with (or immersed in) H_2O_2 water solutions are easily obtained (owing to the negligible Raman scattering of water) the same does not hold for IR spectra, because the large excess water absorb completely the IR radiation and prevents the observation of any $\nu(\text{O-O})$ modes. The latter limitation has been surmounted by removing part of the excess of soaking water, through a suitable vacuum manifold. It will be shown that under these conditions the peroxo species are sufficiently stable to be observed by FTIR spectroscopy during evacuation of the excess H_2O . When made

at RT the same procedure leads to the destruction of the peroxo/hydroperoxo species.

EXPERIMENTAL

TS-1 sample (Ti content 1.47 wt%) was synthesized in the ENICHEM laboratories as described in (1). Transmission IR spectra have been collected at 2 cm^{-1} resolution on a Bruker IFS66 spectrometer equipped with an HgCdTe cryodetector. The sample (in form of self-supporting pellets) was inserted in a suitable quartz cell. During all the IR measurements the cell was permanently attached to a vacuum manifold, allowing the accurate control of both sample temperature and equilibrium pressure of water. The experimental procedure was as follows. The pellets were initially impregnated with H_2O_2 solutions, both neutral and basic, of the desired concentration. Then they were inserted in the IR cell and cooled down to about 110 K. The excess water was then gradually removed by progressively increasing the sample temperature from 110 K to room temperature and by simultaneously decreasing the equilibrium pressure of H_2O through a vacuum manifold permanently attached to the IR cell. This pressure and temperature control does not only allow us to gradually remove the excess of water but also to increase the lifetime of the peroxo complexes (which is unstable *in vacuo*). A series of fast IR spectra (2 interferograms per second) have been collected during evacuation in order to detect the transient manifestations of peroxidic structures. The adoption of this particular experimental procedure has been proved to be indispensable for the observation of the IR spectra of the peroxo/hydroperoxo species which under *vacuo* have a transient character (17,28).

Raman spectra have been collected with a resolution of 2 cm^{-1} on a Perkin-Elmer 2000R-NIR-FT Raman spectrometer equipped with an InGaAs detector and employing a Nd-YAG crystal laser pumped by a high pressure Krypton lamp; the adopted wavelength was 1064 nm and the output power was 1.0 W. The sample, in form of powder, was kept soaked with H_2O_2 solutions, by immersing the lower part of the powder in the solution of interest. In order to limit the heating effect of the laser beam which rapidly causes the decomposition of the peroxidic species a rotating sample holder, cooled down at 230 K, has been used.

The solutions used in the experiments have been obtained by mixing a H_2O_2 solution (52%) with a NH_3 (or NaOH) solution (30%) in a ratio $\text{NH}_3/\text{H}_2\text{O}_2=3$ ($\text{NaOH}/\text{H}_2\text{O}_2=3$).

RESULTS AND DISCUSSION

Spectroscopy

Vibrational spectroscopies (IR and Raman) can provide direct information on the $\nu(\text{O-O})$ stretching modes of

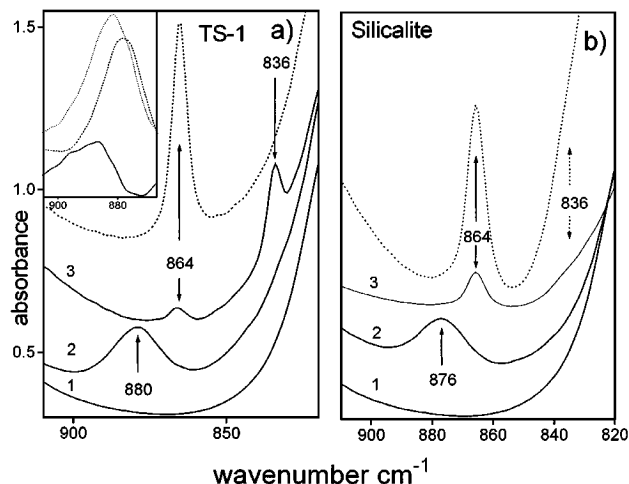


FIG. 1. Influence of ligand dosage in the O-O stretching region as monitored by IR spectroscopy on TS-1 (part a) and on silicalite (part b). Spectra of dehydrated samples (curves 1) after interaction with H₂O₂ sample at about 230 K (curves 2), after contact with a solution of NH₃ and H₂O₂ (NH₃/H₂O₂ = 3) at about 110 K (dotted curves) and after subsequent heating of the sample at about 230 K with parallel continuous decrease of the equilibrium pressure (curves 3). Full arrows indicate the position of observed bands, while the broken arrow in part (b) indicates the position of the 834 cm⁻¹ band, not observed in experiments performed on silicalite. The inset reports superimposed, in a magnified scale, the two re-linearized and renormalized spectra of curves 2 of parts (a) and (b) (dotted and dashed lines, respectively) and corresponding difference (H₂O₂/TS-1 minus H₂O₂/silicalite, full line) which is a well-defined band centered at 886 cm⁻¹.

peroxo complexes and, hence, it is of great utility for elucidating the structure of Ti-peroxo complexes. For the sake of simplicity we will here describe only the IR features in the narrow interval, where the $\nu(\text{O-O})$ modes are expected (Figs. 1a and 1b). Other regions are not informative because, under the adopted experimental conditions, they are heavily dominated by the manifestation of the stretching and bending modes of water, which is the more abundant adsorbate, even under the low pressure conditions adopted in our experiment. As far as the Raman spectra are concerned, a much wider range (1100–800 cm⁻¹) can be studied, since water is a very poor Raman scatterer and, hence, does not appreciably cover the vibrational manifestations of other solutes and adsorbates (Fig. 2).

As far as the effect of H₂O₂/H₂O solution dosage on the characteristic 960 cm⁻¹ band is concerned, little information can be derived from the IR spectra under the adopted experimental conditions, because the transmission in the IR is already critically low in this region due to the combined effect of the high intensity of the 960 cm⁻¹ peak and the water absorption. On the contrary, the Raman spectra (Fig. 2, curves 2 and 3) are very useful and distinctly show a shift to higher frequencies of the peak accompanied by broadening. The same feature is also observed upon pure H₂O dosage (9). This phenomenon is exalted in presence

of the basic NH₃/H₂O₂ solution, but a precise figure of the shift cannot be given because, in this case, the spectrum is made complicated by the presence of overlapping bands due to ammonia oxidation products (see below). Although the shift of the fingerprint band upon the solution contact is clearly indicating the involvement of the Ti centre, it does not give, alone, information on the detailed structure of the peroxo/hydroperoxo complexes. Coming back to the 900–800 cm⁻¹ range several new bands appear in the IR and Raman spectra. All the IR experiments were also duplicated on a pure silicalite sample (bearing the same MFI structure but with a pure SiO₂ composition), in order to single out with certainty the manifestations associated with the Ti centres in the Ti-containing zeolite. The results (Figs. 1 and 2) can be summarized as follows:

(i) Upon dosage, at about 230 K, of neutral H₂O₂ solution on TS-1, a new absorption with the maximum centered at about 880 cm⁻¹ is formed (IR weak, Fig. 1a, curve 2) and 875 cm⁻¹ (Raman intense, Fig. 2, curve 2). Since a similar

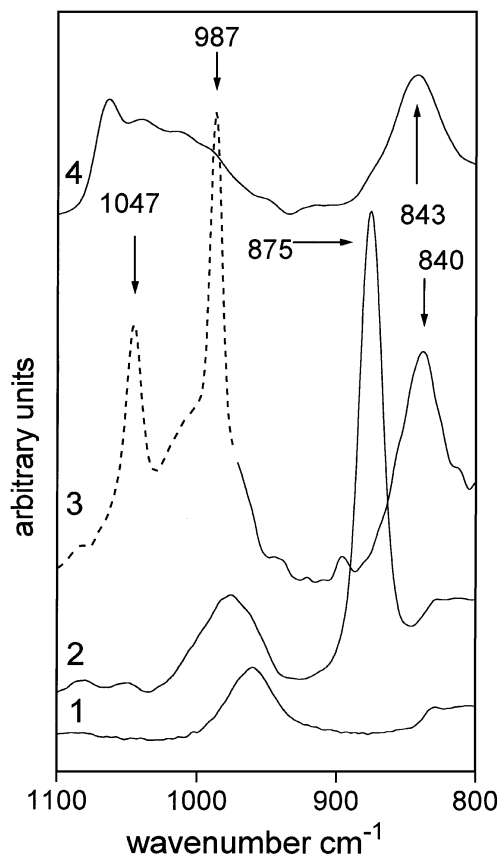


FIG. 2. Influence of ligand dosage in the 1100–800 cm⁻¹ region as monitored by Raman spectroscopy. Curve 1, dehydrated TS-1; curve 2, after interaction with H₂O₂; curve 3, after interaction with NH₃ and H₂O₂ (assignment of bands appearing in the dotted part of spectrum 3 is tentative); curve 4, after interaction with NaOH and H₂O₂. All spectra have been recorded at 230 K.

band at 876 cm^{-1} is also observed on the silicalite (Fig. 1b, curve 2), and since the $\nu(\text{O-O})$ vibration of liquid H_2O_2 is found at 875 cm^{-1} , we conclude that the 880 cm^{-1} (IR) and 875 cm^{-1} (Raman) band mainly results from physisorbed H_2O_2 into TS-1 channels. It is worth noticing that, by comparing the two IR bands obtained by dosing the neutral H_2O_2 solution on TS-1 and on silicalite, beside the shift shown of the maximum of about 4 cm^{-1} , the band obtained on TS-1 has a significantly larger FWHM (about 18 against about 14 cm^{-1}). In order to better appreciate this important fact, the inset of Fig. 1 reports, in a magnified scale, the two relinearized and renormalized spectra (TS-1 and silicalite, dotted and dashed lines, respectively) and corresponding difference (TS-1 minus silicalite, full line). It is now more evident that the IR band on TS-1 has a shoulder at higher frequencies, not present in silicalite, which could be tentatively ascribed to a labile hydroperoxide complex (Ti-OOH), since *ab initio* calculations predict that the $\nu(\text{O-O})$ of such complex should not differ significantly from those of H_2O_2 (HF, 1042.7, Corr., 885.2 cm^{-1} for Ti-OOH ; against HF, 1031.3, Corr., 876.0 cm^{-1} for physisorbed H_2O_2 , see below). Experimentally, the difference spectrum locates the maximum of this additional band (which is quite asymmetric on the high frequency tail) at 886 cm^{-1} . Moreover, a spectral deconvolution (using ASYMGRAD software (30,31)) of the spectrum of the $\text{H}_2\text{O}_2/\text{TS-1}$ system into two gaussian components, the frequency of the former being fixed at 876 cm^{-1} to simulate the $\text{H}_2\text{O}_2/\text{silicalite}$ system, locates the frequency of the latter at 884 cm^{-1} . It is correct to recognize that, due to the strong overlap between the two components and to the nonunivocal choice of the couple of points used to relinearize both spectra, the exact location of the IR band of the labile hydroperoxide complex still remains questionable; however, also supported by our theoretical study, we can safely affirm that upon dosage, at about 230 K, of neutral H_2O_2 solution on TS-1, a hydroperoxide complex (Ti-OOH) is formed in TS-1, whose O-O stretching frequency is few cm^{-1} higher than that of physisorbed H_2O_2 (i.e., somewhere between 890 and 880 cm^{-1}). Unfortunately we cannot support our conclusion with Raman experiments, since the Raman band at 875 cm^{-1} measured when H_2O_2 is dosed on silicalite (not shown for brevity) is very similar to that observed on TS-1 (curve 2 in Fig. 2). The fact that the broadening at higher frequencies is not observed in the Raman experiment is probably due to the heating effect of the laser beam, which, by favoring the decomposition of the complex, keeps its concentration at low level. The negative effect of the laser beam even at 230 K is also confirmed by the decolourized spot formed on the sample where the laser beam strikes the samples.

(ii) Upon interaction, at 230 K, with basic aqueous solutions (the $\text{NH}_3/\text{H}_2\text{O}_2$ or $\text{NaOH}/\text{H}_2\text{O}_2$), two new IR bands are observed on TS-1 (Fig. 1a, curve 3) at 864 and 836 cm^{-1} .

To fully understand the nature of these two new spectroscopic species it is necessary to follow the evolution of the IR spectrum of the basic solution dosed on TS-1 from liquid nitrogen temperature to room temperature under continuous decrease of the equilibrium pressure inside the cell, as described in the experimental section. At a lower temperature (about 110 K) (see dotted curve in Fig. 1a) the intensity of the 864 cm^{-1} band is much greater while the band at 836 cm^{-1} is totally absent; by increasing the sample temperature under pumping the 864 cm^{-1} band continuously decreases, while a new band develops at 836 cm^{-1} , reaching its maximum at about 230 K (see spectrum 3 in Fig. 1a). A further increase of the temperature up to room temperature leads to the total destruction of the 836 cm^{-1} band, while only a vestige of the of the 864 cm^{-1} band survives. The absence of the 836 cm^{-1} band in the “as cooled” spectrum (dotted curve in Fig. 1a) is due to the presence of a still-significant excess of adsorbed water in the adopted experimental conditions. In fact, H_2O deeply perturb the Ti-OOH complex by strong hydrogen bond interactions, resulting in a great broadening of the O-O band which does not emerge any more from the left-hand side of the strong IR absorption due to the SiO_2 modes centered at about 800 cm^{-1} . The fundamental role of our the apparently exotic experimental procedure adopted in this investigation is now evident, since a prolonged outgassing at liquid nitrogen temperature is not sufficient to remove, in a significant way, adsorbed water and a parallel temperature increase is consequently necessary. Unfortunately this procedure has a concomitant but opposite effect because it is associated with the reduction of the hydroperoxo complex stability. On the basis on a series of experiments the 230 K temperature has been observed to be the best one to allow the observation of this O-O stretching.

To further confirm our assignment, we have performed the same experiments by dosing the basic aqueous solutions ($\text{NH}_3/\text{H}_2\text{O}_2$ or $\text{NaOH}/\text{H}_2\text{O}_2$) on silicalite. They yield only to the formation of the species adsorbing at 864 cm^{-1} , which behavior upon increasing the sample temperature and decreasing the equilibrium pressure is fully parallel to the same band observed on TS-1, see dotted spectrum and spectrum 3 of Fig. 1b. In the investigated temperature range (between 110 and 300 K) no band around 836 cm^{-1} was detected. While the 864 cm^{-1} band is also observed on Silicalite and it is readily assigned to $\nu(\text{O-O})$ of $\text{NH}_4^+\text{OOH}^-$, it is evident that the band at 836 cm^{-1} must represent a true fingerprint of the more stable complex formed in basic conditions. In full agreement with the IR study, it must be stressed that a similar band is also observed at about 230 K, in the Raman experiment, both with $\text{NH}_3/\text{H}_2\text{O}_2$ (at 840 cm^{-1}) and $\text{NaOH}/\text{H}_2\text{O}_2$ (at 843 cm^{-1}) solutions (see Fig. 2, curves 3 and 4, respectively). The fact that the $836\text{--}843\text{ cm}^{-1}$ band appears also in the experiments where

the NaOH/H₂O₂ solution is used discards any possible assignment in terms of a vibrational mode of an unknown product of the oxidative chemistry of NH₃.

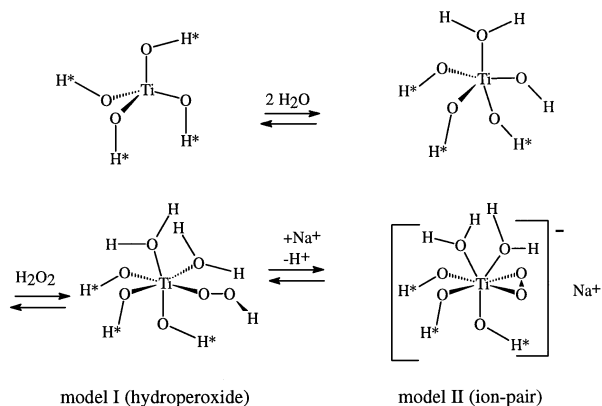
(iii) New Raman bands appear also at 987 cm⁻¹ and 1047 cm⁻¹ (part of the spectrum reported as the dotted line), which are plausible, related to the oxidative chemistry of NH₃. The intensity of these two bands is variable from one experiment to the other, and their attribution is only tentative. The 1047 cm⁻¹ band can be assigned to NO₃⁻ species resulting from ammonia oxidation. As far as the 987 cm⁻¹ band, an attribution is less straightforward. A plausible assignment to NH₂OH (whose formation is known to be catalyzed by TS-1 (15)) is excluded, since the adsorption of a NH₂OH solution on the structural isomorphous silicalite originates an IR peak at 911 cm⁻¹. A possible candidate can be identified in NH₃OH⁺ Z⁻ species (where Z⁻ is the TiOO⁻), since the dosage of hydroxylamine chloride (NH₃OHCl) on silicalite produces an absorption at 998 cm⁻¹ (spectrum not reported for brevity). Following this hypothesis hydroxylamine once formed by oxidation of NH₃ at the Ti centres, is under a salt-like form.

It is worth noticing that Clerici *et al.*, in their pioneering work (28) already discussed the presence of stable peroxide complexes in TS-1 under basic media (LiOH, NaOH, KOH, AcONa); they report that the molar ratio of peroxide species per Ti center increases with the strength and with the concentration of the base. Even if no IR spectra are shown, they discuss the results of IR experiments on such basic solutions by mainly analyzing quantitatively the erosion of the fingerprint band at 960 cm⁻¹ (indicated at 970 cm⁻¹ in that work) upon increasing the concentration of the LiOH base, see Table 4 in Ref. (28). It must, however, be underlined that the erosion of the 960 cm⁻¹ band, together with a small blue-shift, is not peculiar of peroxide complexes formed on Ti, since it is systematically observed upon dosing ligands like NH₃, H₂O, etc. on TS-1 (see the Introduction). They also report the presence of an "extra peak" at 866 cm⁻¹ in spectra of peroxides prepared with a LiOH concentration greater than 0.1 M; however, no assignment is given by the authors. No other bands are described; this means that Clerici *et al.*, were not able to detect the fundamental 836 cm⁻¹ band. This is not surprising, since we have shown that the interesting peroxidic specie disappears upon drying the sample at room temperature and that the sophisticated experimental procedure, described before, is indispensable to detect this key species. It is evident that the "extra peak" observed by Clerici *et al.*, being at a very similar frequency (866 against 864 cm⁻¹) to that of the band assigned by us to the NH₄⁺OOH⁻ specie, is probably due to the Li⁺OOH⁻ complex. In this regard please note also that our parallel experiment locates the frequency of the Na⁺OOH⁻ complex at 864 cm⁻¹.

In conclusion, the vibrational experiments presented here suggest the possible existence, under neutral conditions, of an unstable Ti complex containing the O-O moiety (plausibly an OOH group) absorbing at frequencies slightly higher than physisorbed H₂O₂ (tentatively in the 890–880 cm⁻¹ range) and responsible for the already measured UV-Vis absorption at 25800 cm⁻¹ (15,17,19). This species can be transformed in basic conditions into a more stable form, absorbing at 840 cm⁻¹ (Raman) and 836 cm⁻¹ (IR), responsible of the UV-Vis edge at 28500 cm⁻¹ (15,17,19). A structural model for these complexes, based on *ab initio* quantum chemical calculations, is given in the following section.

Ab Initio Calculations

Ab initio quantum chemical calculations on cluster models of catalytic sites have proved to be an increasingly accurate method for the prediction of the structures and spectroscopic features of catalytic centres, provided that the adopted clusters are appropriately constructed and that the effect of the neglected embedding solid are kept in mind. Previous theoretical studies have already addressed the problem of the structure of the Ti centre (17,26,32–38) and of its interaction with H₂O (35,37) with different models and methods. Recently, the interaction of tetrahedrally coordinated Ti with H₂O₂ has also been addressed (38). The calculations presented here represent a strongly improved version of the preliminary results very briefly discussed in Ref. (17). The scope of these calculations is limited to the study of the structure and vibrational frequencies of the smallest possible model for the active centre, resulting from the interaction of the native tetrahedral Ti centre with water ligands and H₂O₂. The energetics of these interactions is a more complex topic, on which scarce experimental data are available, and it will not be discussed in detail here. The model contains the first shell of atoms neighboring with Ti and can be thought as resulting from the following reaction, where the OH* groups model the O-Si connections with the zeolite framework.



Initially a H_2O molecule coordinates to Ti(IV) while a second H_2O molecule hydrolyzes a Ti-O-Si bridge,¹ then the reaction goes on with H_2O_2 , forming the hydroperoxide species and a second water ligand which coordinates to Ti(IV) . In the presence of Na^+ ions the hydroperoxide is converted to an ionic ion pair.

The geometry of models 1 (hydroperoxide) and 2 (ion-pair) has been optimized, with particular care devoted to the detection of multiple configurations related to η^1 (monodentate or edge-on) or η^2 (bidentate or side-on) coordination of the peroxide/hydroperoxide ion. To this purpose, each cluster model was optimized with two different initial geometries corresponding to hypothetical η^1 and η^2 geometry. For each local minimum energy configuration found, vibrational frequencies were calculated (harmonic approximation) to confirm its nature and to be compared with the experimental data. All the calculations were done with the Gaussian92 code (39) at the Hartree-Fock level using a valence double zeta basis set (VDZ) (40). Different η^1 and η^2 initial geometries were tried. Optimized structures are shown in Fig. 3.

For the hydroperoxide model only one type of minimum was found, with η^1 coordination (Fig. 3, part a). This is in contrast with the results of Ref. (38), but the discrepancy can be explained by the fact that the model adopted in Ref. (38) assumes a sterically less crowded five-coordinated Ti centre. In the minimized structure the O-H^* groups are 1.8 Å apart from the Ti(IV) centre, the Ti-O distance in coordinated water molecules is 2.1–2.2 Å, the $\eta^1\text{-OOH}$ group bounds less strongly than O-H^* to the Ti centre ($d(\text{Ti-O}) = 2.00$ Å), and it forms a strong hydrogen bond with H_2O molecules also coordinated to Ti ($d(\text{H-O}) = 1.68$ Å).

For the Na ion pair models, two distinct local minima were identified, one with η^1 and the second with η^2 coordination of the OO^{2-} anion. The energy of the η^2 complex is found to be 35.4 kJ/mol lower than that of the η^1 (this value is in qualitative good agreement with the preliminary value of 10.5 kcal/mol \approx 43.9 kJ/mol reported in (17)). In both η^1 and η^2 structures, the Na^+ ion is coordinated to the peroxide ion and to a Ti-OH^* group. Also in this case the Ti-O distance in coordinated water molecules is observed to be 2.1–2.2 Å, while the distance to the oxygen in OH^* groups is always around 1.8 Å (this value is in complete agreement with experimental data obtained by EXAFS (13,14,23–25)).

It is worth noticing that it would be of great interest to confirm, from a computational approach, the spectroscopic evidence that the peroxo complexes formed in basic me-

¹ Please note how, from a stoichiometric point of view, in the right-hand term of the first reaction a H-O-H^* is missing. It represents the silanol of the adjacent T site formed after the hydrolyzation of the second H_2O molecule (see upper part of the first scheme). Its absence is due to the fact that in the second scheme only atoms belonging to the investigated clusters are represented.

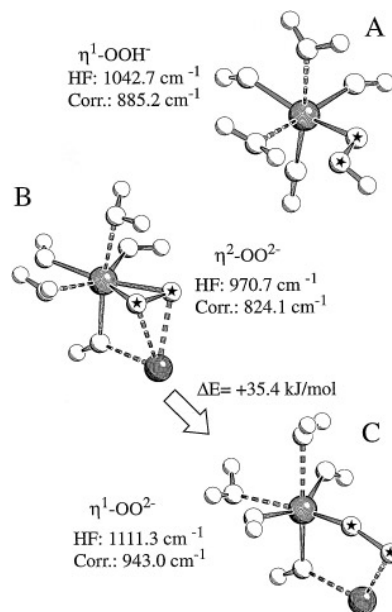


FIG. 3. Selected structural and vibrational features of the optimized cluster models. (A) η^1 hydroperoxide complex; (B) Na containing η^1 ion pair complex; (C) Na containing η^2 ion pair complex. $\nu(\text{O-O})$ calculated frequencies are also reported (see text). Structure (B) (η^2) is more stable than structure (C) (η^1) by 35.44 kJ/mol. For the three parts big and small white spheres represents O and H atoms, respectively, while the central black sphere is Ti; oxygen atoms coming from H_2O_2 are marked with a black star. In parts (B) and (C) the added black spheres represent sodium. Solid sticks are chemical bonds, while broken sticks link coordinated species.

dia have a higher stability with respect to that formed in a neutral condition. From a stoichiometric point of view, it is evident that this further proof could be derived by studying the reaction of complex A + NaOH (or $\text{A} + \text{NH}_3$), which gives complex B + H_2O (or complex B with NH_4^+ , instead of Na^+). This point is very interesting; however, the calculation of the energy for such reactions is not trivial and it is beyond the scope of this paper. In fact, while the reaction of the sodium-form is not clearly defined (would the NaOH ion pair be one of the reactants?), the reaction with ammonia requires nontrivial additional calculations. Moreover, the chemistry of the complex with $\text{NH}_3/\text{NH}_4^+$ would be characterized by complex H-bond interactions with the terminating OH^* groups of the cluster and H_2O . A bigger model, including the next SiO_4 tetrahedra, or an embedded model, would clearly be needed. This subject is complex enough to require a study on its own. For this reason we report only the energy difference between the two forms of the ion pair complexes (forms B and C).

Please note that these are precisely the computational reasons why we decided to perform our *ab initio* calculations on ion-pair models (forms A and B) using Na^+ instead of NH_4^+ as cation, also supported by the experimental evidence that $\text{NH}_3/\text{H}_2\text{O}_2$ and $\text{NaOH}/\text{H}_2\text{O}_2$ solutions dosed

on TS-1 give rise to nearly indistinguishable spectroscopic features in the O-O stretching region (see above).

The vibrational spectra for the three structures were calculated in order to compare with the experimental observation of stretching O-O vibrations. With the aim to correct the well-known overestimation of vibrational frequencies by the Hartree-Fock method, a scaling factor of 0.849 was applied. This value differs slightly from the generally accepted scaling constant (0.89) and results from the ratio between the experimentally observed $\nu(\text{O-O})$ of liquid H_2O_2 in silicalite (876 cm^{-1}) and the calculated value for an isolated H_2O_2 molecule (1031.4 cm^{-1}). Solvation effects due to the zeolitic wall are thus included, although in a crude way, in the scaling factor. In the following, uncorrected calculated frequencies are given in parenthesis after the abbreviation "HF," while scaled values are preceded by "Corr."

The $\nu(\text{O-O})$ frequency of the η^1 hydroperoxide (Fig. 3a) complex (HF, 1042.7 ; Corr., 885.2 cm^{-1}) are similar to the values observed when H_2O_2 is dosed on silicalite (Fig. 1a, spectrum 2) and that calculated for unperturbed H_2O_2 molecule. The predicted upward shift upon coordination is 10 cm^{-1} , while the observed shift of the band maximum accounts for $\sim 4\text{ cm}^{-1}$. This value is inferred from the maximum of a relatively broad band also containing the contribution of physisorbed H_2O_2 ; when a careful subtraction of the band obtained on silicalite from that obtained on TS-1 is done, a band appears at 886 cm^{-1} , i.e. very close to the computational frequency. The same holds when a deconvolution into two components is done; see above.

As far as the ion-pair models are concerned (Figs. 3b and 3c), the $\nu(\text{O-O})$ of the η^1 complex is calculated to be strongly IR active and *poorly Raman active* at (HF, 1111.3 cm^{-1} ; Corr., 943 cm^{-1}). Since we do not observe IR manifestations near this frequency (emerging from the framework stretching modes) and since the Raman peak observed at 987 cm^{-1} is very strong and can be otherwise explained (see before), we will discard the hypothesis of an η^1 complex. This conclusion is also supported by the higher energy calculated for this structure (see above). On the contrary, the $\nu(\text{O-O})$ frequency calculated for the η^2 complex (Fig. 3b) (HF, 970.7 cm^{-1} ; Corr., 824.1 cm^{-1}) is in good agreement with the observed frequencies (IR, 836 cm^{-1} ; Raman, 840 cm^{-1}).

CONCLUSIONS

The structure of the complexes formed upon interaction of the Ti catalytic centre in TS-1 with hydrogen peroxide water solutions has been studied by spectroscopic and computational methods. Upon interaction with neutral aqueous H_2O_2 solutions, the formation of an unstable hydroperoxidic species, previously evidenced by UV-Visible spectroscopy (absorption at 25800 cm^{-1}) (15,17,19) absorbing at a frequency near to that of the uncomplexed H_2O_2 (tentatively in the $890\text{--}880\text{ cm}^{-1}$ range) has been inferred. On the contrary, in a basic environment, the hy-

droperoxo complex is converted into a more stable ionic one which shows peculiar O-O stretching bands at 836 cm^{-1} (IR) and at 840 cm^{-1} (Raman); this complex is responsible of the already observed UV-Vis absorption at 25800 cm^{-1} (15,17,19). It is important to stress that the adoption of an original experimental procedure involving low temperature measurements and accurate control of the H_2O equilibrium pressure is the most relevant part of this work, indispensable in the delicate spectroscopic detection of an elusive and unstable species (as normally expected for a structure playing a key role in catalysis).

The assignment of the spectra has been confirmed by parallel experiments on the structurally similar Ti-free silicalite and by *ab initio* calculations. The study of the structure and of the vibrational frequencies of the smallest model of the active center (ion pair) indicates that the ion pair η^2 complex is the most stable and is characterized by a calculated $\nu(\text{O-O})$ in good agreement with the experimental IR and Raman results.

REFERENCES

1. Taramasso, M., Perego, G., and Notari, B., U.S. Patent 4,410,501 (1983).
2. Neri, C., Esposito, A., Anfossi, B., and Buonomo, F., Europ. Patent 100,119 (1984).
3. Neri, C., Anfossi, B., and Buonomo, F., Europ. Patent 100,118 (1984).
4. Esposito, A., Neri, C., and Buonomo, F., Europ. Patent 4,480,135 (1984).
5. Esposito, A., Taramasso, M., Neri, C., and Buonomo, F., Brit. Patent 2,116,974 (1985).
6. Roffia, P., Padovan, M., Moretti, E., and De Alberti, G., Europ. Patent 208,311 (1987).
7. Roffia, P., Padovan, M., Leofanti, G., Mantegazza, M. A., De Alberti, G., and Tanszik, G. R., U.S. Patent 4,794,198 (1988).
8. Bellussi, G., Carati, A., Clerci, G. M., Maddinelli, G., and Millini, R., *J. Catal.* **133**, 220 (1992).
9. Scarano, D., Zecchina, A., Bordiga, S., Geobaldo, F., Spoto, G., Petrini, G., Leofanti, G., Padovan, M., and Tozzola, G., *J. Chem. Soc., Faraday Trans.* **89**, 4123 (1993).
10. Perego, G., Bellussi, G., Corno, C., Taramasso, M., Buonomo, F., and Esposito, A., *Stud. Surf. Sci. Catal.* **28**, 129 (1986).
11. Huybrechts, D. R. C., Buskens, P. L., and Jacobs, P. A., *J. Mol. Catal.* **71**, 129 (1992).
12. Boccuti, M. R., Rao, K. M., Zecchina, A., Leofanti, G., and Petrini, G., *Stud. Surf. Sci. Catal.* **48**, 133 (1989).
13. Bordiga, S., Coluccia, S., Lamberti, C., Marchese, Zecchina, A., Boscherini, F., Buffa, F., Genoni, F., Leofanti, G., Petrini, G., and Vlaic, G., *J. Phys. Chem.* **98**, 4125 (1994).
14. Bordiga, S., Coluccia, S., Lamberti, C., Marchese, L., Boscherini, F., Genoni, F., Leofanti, G., Petrini, G., Vlaic, G., and Zecchina, A., *Catal. Lett.* **26**, 195 (1994).
15. Zecchina, A., Spoto, G., Bordiga, S., Geobaldo, F., Petrini, G., Leofanti, G., Padovan, M., Mantegazza, M., and Roffia, P., in "New Frontiers in Catalysis" (L. Gucci, F. Solymosi, and P. Tètényi, Eds.), p. 719. Akad. Kiadó, Budapest, 1993.
16. Zecchina, A., Spoto, G., Bordiga, S., Padovan, M., Leofanti, G., and Petrini, G., *Stud. Surf. Sci. Catal.* **65**, 671 (1991).
17. Zecchina, A., Bordiga, S., Lamberti, C., Ricchiardi, G., Scarano, D., Leofanti, G., Petrini, G., and Mantegazza, M., *Catal. Today* **32**, 97 (1996).
18. Notari, B., *Adv. Catal.* **41**, 253 (1996).

19. Geobaldo, F., Bordiga, S., Zecchina, A., Giamello, E., Leofanti, G., and Petrini, G., *Catal. Lett.* **16**, 109 (1992).
20. Millini, R., Previde-Massara, E., Perego, G., and Bellussi, G., *J. Catal.* **137**, 497 (1992).
21. Trong On, D., Bittar, A., Sayari, A., Bonnevot, L., and Kaliaguine, S., *Catal. Lett.* **16**, 85 (1992).
22. Ruiz-Lopez, M. F., and Munoz-Paez, A., *J. Phys. Condens. Matter* **3**, 9881 (1991).
23. Le Noc, L., Trong On, D., Solomykina, S., Echchahed, B., Béland, F., Cartier dit Moulin, C., and Bonnevot, L., *Stud. Surf. Sci. Catal.* **101**, 611 (1996).
24. Lamberti, C., Bordiga, S., Zecchina, A., Vlaic, G., Tozzola, G., Petrini, G., and Carati, A., *J. Phys. IV France* **7**, C2-851 (1997).
25. Lamberti, C., Bordiga, S., Arduino, D., Zecchina, A., Geobaldo, F., Spanò, G., Genoni, F., Petrini, G., Carati, A., Villain, F., and Vlaic, G., *J. Phys. Chem. B* **102** (1998).
26. Jentys, A., and Catlow, C. R. A., *Catal. Lett.* **22**, 251 (1993).
27. Clerici, M. G., and Ingallina, P., *J. Catal.* **140**, 71 (1993).
28. Clerici, M. G., Ingallina, P., and Millini, R., in "Proc. 9th Int. Zeolite Conf., Montreal, 1992" (R. von Ballmoos, J. B. Higgins, and M. M. J. Treacy, Eds.), p. 445. Butterworth-Heinemann, Stoneham, MA, 1993.
29. Mantegazza, M. A., Leofanti, G., Petrini, G., Padovan, M., Zecchina, A., and Bordiga, S., *Stud. Surf. Sci. Catal.* **82**, 541 (1994).
30. Lamberti, C., Bordiga, S., Cerrato, G., Morterra, C., Scarano, D., Spoto, G., and Zecchina, A., *Comput. Phys. Commun.* **74**, 119 (1993).
31. Lamberti, C., Morterra, C., Bordiga, S., Cerrato, G., and Scarano, D., *Vibr. Spectrosc.* **4**, 273 (1993).
32. Millini, R., Perego, G., and Seiti, K., *Stud. Surf. Sci. Catal.* **84**, 2123 (1994).
33. de Man, A. J. M., and Sauer, J., *J. Phys. Chem.* **100**, 5025 (1996).
34. Zicovich-Wilson, C., and Dovesi, R., *Nuovo Cimento D* **19**, 1785 (1997).
35. Zicovich-Wilson, C., and Dovesi, R., *J. Mol. Catal.* **119**, 449 (1997).
36. Zicovich-Wilson, C., and Dovesi, R., *J. Phys. Chem. B* **102**, 1411 (1998).
37. Sinclair, P. E., Sankar, G., Catlow, C. R. A., Thomas, J. M., and Maschmeyer, T., *J. Phys. Chem. B* **101**, 4232 (1997).
38. Karlsen, E., and Schöffel, K., *Catal. Today* **32**, 107 (1996).
39. Frisch, M. J., Trucks, G. W., Schlegel, H. B., Gill, P. M. W., Johnson, B. G., Wong, M. W., Foresman, J. B., Robb, M. A., Head-Gordon, M., Replogle, E. S., Gomperts, R., Andres, J. L., Raghavachari, K., Binkley, J. S., Gonzalez, C., Martin, R. L., Fox, D. J., Defrees, D. J., Baker, J., Stewart, J. J. P., and Pople, J. A., Gaussian 92/DFT, Revision G3, Gaussian, Inc., Pittsburgh, PA, 1993.
40. Schafer, A., Horn, H., and Ahlrichs, R., *J. Chem. Phys.* **97**, 2571 (1992).